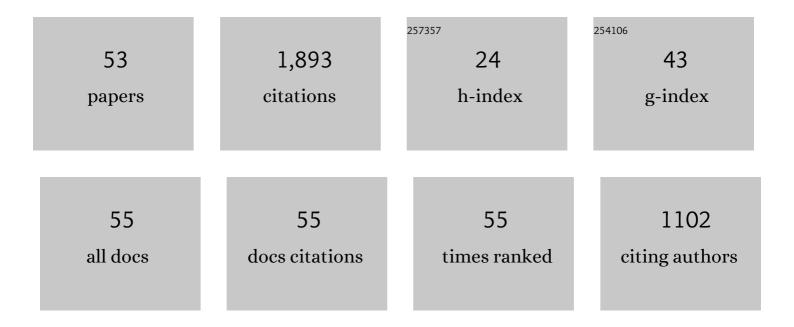
Gopi K Seemala

List of Publications by Year in descending order

Source: https://exaly.com/author-pdf/4162919/publications.pdf Version: 2024-02-01



#	Article	IF	CITATIONS
1	Statistics of total electron content depletions observed over the South American continent for the year 2008. Radio Science, 2011, 46, .	0.8	260
2	Temporal and spatial variations in TEC using simultaneous measurements from the Indian GPS network of receivers during the low solar activity period of 2004–2005. Annales Geophysicae, 2006, 24, 3279-3292.	0.6	221
3	Local time dependent response of postsunset ESF during geomagnetic storms. Journal of Geophysical Research, 2008, 113, .	3.3	86
4	Study of spatial and temporal characteristics of L-band scintillations over the Indian low-latitude region and their possible effects on GPS navigation. Annales Geophysicae, 2006, 24, 1567-1580.	0.6	83
5	Geomagnetic storm effects on GPS based navigation. Annales Geophysicae, 2009, 27, 2101-2110.	0.6	81
6	Equatorial plasma bubbles and L-band scintillations in Africa during solar minimum. Annales Geophysicae, 2012, 30, 675-682.	0.6	75
7	Assessment of the NeQuick-2 and IRI-Plas 2017 models using global and long-term GNSS measurements. Journal of Atmospheric and Solar-Terrestrial Physics, 2018, 170, 1-10.	0.6	60
8	Comparison of equatorial GPS-TEC observations over an African station and an American station during the minimum and ascending phases of solar cycle 24. Annales Geophysicae, 2013, 31, 2085-2096.	0.6	58
9	Threeâ€dimensional GPS ionospheric tomography over Japan using constrained least squares. Journal of Geophysical Research: Space Physics, 2014, 119, 3044-3052.	0.8	58
10	Electrodynamic disturbances in the Brazilian equatorial and lowâ€latitude ionosphere on St. Patrick's Day storm of 17 March 2015. Journal of Geophysical Research: Space Physics, 2017, 122, 4553-4570.	0.8	57
11	Features of additional stratification in ionospheric F 2 layer observed for half a solar cycle over Indian low latitudes. Journal of Geophysical Research, 2005, 110, .	3.3	50
12	VHF and L-band scintillation characteristics over an Indian low latitude station, Waltair (17.7Ű N, 83.3Ű) Tj ETQ	q0.0.0 rgB 0.6	BT /Qverlock
13	Medium-scale traveling ionospheric disturbances by three-dimensional ionospheric GPS tomography. Earth, Planets and Space, 2016, 68, .	0.9	47
14	Twoâ€mode ionospheric response and Rayleigh wave group velocity distribution reckoned from GPS measurement following <i>M_w</i> 7.8 Nepal earthquake on 25 April 2015. Journal of Geophysical Research: Space Physics, 2015, 120, 7049-7059.	0.8	45
15	A comparative study of TEC response for the African equatorial and mid-latitudes during storm conditions. Journal of Atmospheric and Solar-Terrestrial Physics, 2013, 102, 105-114.	0.6	44
16	Simultaneous observations of ionospheric irregularities in the African low-latitude region. Journal of Atmospheric and Solar-Terrestrial Physics, 2013, 97, 50-57.	0.6	42
17	On the performance of the IRIâ€2012 and NeQuick2 models during the increasing phase of the unusual 24th solar cycle in the Brazilian equatorial and low″atitude sectors. Journal of Geophysical Research: Space Physics, 2014, 119, 5087-5105.	0.8	41

A Hybrid Regressionâ€Neural Network (HRâ€NN) Method for Forecasting the Solar Activity. Space1.340Weather, 2018, 16, 1424-1436.

GOPI K SEEMALA

#	Article	IF	CITATIONS
19	A Neural Networkâ€Based Ionospheric Model Over Africa From Constellation Observing System for Meteorology, Ionosphere, and Climate and Ground Global Positioning System Observations. Journal of Geophysical Research: Space Physics, 2019, 124, 10512-10532.	0.8	40
20	GPS-TEC variations during low solar activity period (2007–2009) at Indian low latitude stations. Astrophysics and Space Science, 2012, 339, 165-178.	0.5	38
21	Conjugate hemisphere ionospheric response to the St. Patrick's Day storms of 2013 and 2015 in the 100ŰE longitude sector. Journal of Geophysical Research: Space Physics, 2016, 121, 11,364.	0.8	30
22	Simultaneous storm time equatorward and poleward largeâ€scale TIDs on a global scale. Geophysical Research Letters, 2016, 43, 6678-6686.	1.5	30
23	Signatures of Equatorial Plasma Bubbles and Ionospheric Scintillations from Magnetometer and GNSS Observations in the Indian Longitudes during the Space Weather Events of Early September 2017. Remote Sensing, 2022, 14, 652.	1.8	28
24	Characterization of GNSS scintillations over Lagos, Nigeria during the minimum and ascending phases (2009–2011) of solar cycle 24. Advances in Space Research, 2014, 53, 37-47.	1.2	26
25	Multifractal detrended fluctuation analysis of ionospheric total electron content data during solar minimum and maximum. Journal of Atmospheric and Solar-Terrestrial Physics, 2016, 149, 31-39.	0.6	26
26	Morphological and spectral characteristics of L-band and VHF scintillations and their impact on trans-ionospheric communications. Earth, Planets and Space, 2006, 58, 895-904.	0.9	23
27	Stormâ€īime Modeling of the African Regional Ionospheric Total Electron Content Using Artificial Neural Networks. Space Weather, 2020, 18, e2020SW002525.	1.3	23
28	NeQuick bottomside analysis at low latitudes. Journal of Atmospheric and Solar-Terrestrial Physics, 2008, 70, 1911-1918.	0.6	21
29	Solar quiet current response in the African sector due to a 2009 sudden stratospheric warming event. Journal of Geophysical Research: Space Physics, 2016, 121, 8055-8065.	0.8	21
30	Climatology of GPS amplitude scintillations over equatorial Africa during the minimum and ascending phases of solar cycle 24. Astrophysics and Space Science, 2015, 357, 1.	0.5	19
31	Groundâ€Based GNSS and C/NOFS Observations of Ionospheric Irregularities Over Africa: A Case Study of the 2013ÂSt. Patrick's Day Geomagnetic Storm. Space Weather, 2021, 19, e2020SW002631.	1.3	16
32	Spatial distribution of ionization in the equatorial and low-latitude ionosphere of the Indian sector and its effect on the pierce point altitude for GPS applications during low solar activity periods. Journal of Geophysical Research, 2007, 112, n/a-n/a.	3.3	14
33	Ionospheric Plasma Response to M w 8.3 Chile Illapel Earthquake on September 16, 2015. Pure and Applied Geophysics, 2016, 173, 1451-1461.	0.8	13
34	On the occurrence and strength of multi-frequency multi-GNSS Ionospheric Scintillations in Indian sector during declining phase of solar cycle 24. Advances in Space Research, 2018, 61, 1761-1775.	1.2	13
35	Reconstruction of Stormâ€Time Total Electron Content Using Ionospheric Tomography and Artificial Neural Networks: A Comparative Study Over the African Region. Radio Science, 2018, 53, 1328-1345.	0.8	13
36	Magnetic Conjugacy of Pc1 Waves and Isolated Proton Precipitation at Subauroral Latitudes: Importance of Ionosphere as Intensity Modulation Region. Geophysical Research Letters, 2021, 48, e2020GL091384.	1.5	10

GOPI K SEEMALA

#	Article	IF	CITATIONS
37	Reckoning ionospheric scintillation S4 from ROTI over Indian region. Advances in Space Research, 2022, 69, 915-925.	1.2	10
38	lonospheric disturbances in a large area of the terrestrial globe by two strong solar flares of September 6, 2017, the strongest space weather events in the last decade. Advances in Space Research, 2020, 66, 1775-1791.	1.2	9
39	L-band scintillation and TEC variations on St. Patrick's Day storm of 17 March 2015 over Indian longitudes using GPS and GLONASS observations. Journal of Earth System Science, 2019, 128, 1.	0.6	8
40	Equatorial and low-latitude positive ionospheric phases due to moderate geomagnetic storm during high solar activity in January 2013. Advances in Space Research, 2019, 64, 995-1010.	1.2	7
41	Interhemispheric comparison of the ionosphere and plasmasphere total electron content using CPS, radio occultation and ionosonde observations. Advances in Space Research, 2021, 68, 2339-2353.	1.2	7
42	Ionospheric Plasma Response to M w 8.3 Chile Illapel Earthquake on September 16, 2015. , 2017, , 145-155.		7
43	Characterization of ionospheric total electron content data using wavelet-based multifractal formalism. Chaos, Solitons and Fractals, 2020, 134, 109653.	2.5	6
44	Evidence for the Significant Differences in Response Times of Equatorial Ionization Anomaly Crest Corresponding to Plasma Fountains During Daytime and Post‧unset Hours. Journal of Geophysical Research: Space Physics, 2021, 126, e2020JA028628.	0.8	6
45	Daily and Monthly Variations of the Equatorial Ionization Anomaly (EIA) Over the Brazilian Sector During the Descending Phase of the Solar Cycle 24. Journal of Geophysical Research: Space Physics, 2020, 125, e2020JA027906.	0.8	5
46	Responses of various types of antennas to the globally distributed air-earth current monitored at Maitri, Antarctica. Polar Science, 2021, 30, 100657.	0.5	5
47	New results of ionospheric total electron content measurements from a low-cost global navigation satellite system receiver and comparisons with other data sources. Advances in Space Research, 2021, 68, 3835-3845.	1.2	5
48	GPS TEC variations under quiet and disturbed geomagnetic conditions during the descending phase of 24th solar cycle over the Indian equatorial and low latitude regions. Advances in Space Research, 2021, 68, 1836-1849.	1.2	4
49	On the latitudinal variation in OI 630.0Ânm dayglow emissions in response to the equatorial electrodynamic processes and neutral winds. Advances in Space Research, 2022, 69, 926-938.	1.2	4
50	Geomagnetic activity control on VHF scintillations over an Indian low latitude station, Waltair (17.7‡N, 83.3‡E, 20‡N dip). Journal of Earth System Science, 2005, 114, 437-441.	0.6	3
51	Latitudinal variation in the occurrence of GPS L-band scintillations associated with the day-to-day changes in TEC, h′F and the E×B drift velocity and their impact on GPS satellite signals. Journal of Earth System Science, 2015, 124, 497-513.	0.6	3
52	An experimental investigation into the possible connections between the zonal neutral wind speeds and equatorial plasma bubble drift velocities over the African equatorial region. Journal of Atmospheric and Solar-Terrestrial Physics, 2021, 220, 105663.	0.6	2
53	Three-dimensional ionosphere tomography with GPS-TEC from GEONET in Japan. , 2014, , .		0